Estimating epikarst water storage by time-lapse surface to depth gravity measurements

Cédric Champollion[1], Sabrina Deville[1], Jean Chery[1], Erik Doerflinger[1], Nicolas Le Moigne[1], Roger Bayer[1], Philippe Vernant[1], Naomi Mazzilli[2]

[1] Géosciences Montpellier, CNRS, Univ, Montpellier, UA, Montpellier, France
[2] UMR 1114 EMMAH (UAPV/INRA), Université d'Avignon et des Pays de Vaucluse, Avignon, France.

Accepted *date*. Received *date*; in original form *date*

Abstract:
The magnitude of epikarstic water storage variation is evaluated in various karst settings using a relative spring gravimeter. Gravity measurements are performed during one year and half at the surface and inside caves at different depths on three karst hydro-systems in southern France: two limestone karst systems and one dolomite karst system. We find that significant water storage variations occur in the first ten meters of karst unsaturated zone. The subsurface water storage is also evidenced by complementary magnetic resonance sounding. The comparison between sites of the depth gravity measurements with respect of net water inflow suggests that seasonal water storage depends on the lithology. The transmissive function of the epikarst at the seasonal scale has been deduced from the water storage change estimation. Long (> 6 months) and short (< 6 months) transfer time are revealed in the dolomite and in the limestone respectively.

1) **Introduction**

Despite the large areas of carbonate karst systems in the Mediterranean area, their associated water resources and vulnerability remain poorly known. In a context of climate change and population increase, the karstic areas are becoming key water resources. A better knowledge of the properties of the karst reservoir is therefore needed to manage and protect the resources (Bakalowicz, 2005). Increasing the knowledge of karst hydrogeological properties and functioning is not a simple task. Indeed, a karstified area is complex and spatially heterogeneous with a non-linear response to rainfall. Numerous in-situ field observations lead to the identification of three karst horizons: epikarst, infiltration zone and saturated zone. The epikarst has been first defined by Mangin (1975) as the part of the underground in interaction with the soil and the atmosphere. It is often described as a highly altered zone with a high porosity. In many cases, the epikarst is thought to be a significant water reservoir (Lastennet & Mudry, 1997; Perrin et al., 2003; Klimchouk, 2004; Williams, 2008). Chemically based modeling studies suggest that the epikarst or the infiltration zone could contribute to the total flow discharge at the spring from 30% to 50% (Batiot et al., 2003; Emblanch et al., 2003). This view drastically differs from other studies that attribute most of the discharge to a deeper storage (Mangin, 1975; Fleury et al., 2007). As the epikarst is also vulnerable to potential surface pollution, a better understanding of its hydrological behavior is welcome for an optimal management and protection of water resource and biological activity.

The studies about the karst water transfer and storage are generally based on chemical analysis, borehole measurements and spring hydrograph often used to constrain numerical models (Pinault et al., 2001; Hu et al., 2008; Zhang et al., 2011). Spring chemistry or flow approaches provide useful information at basin scale but limited knowledge about the spatial distribution of hydrogeological properties. On the opposite, borehole measurements provide useful quantitative information but relevant only for the near field scale because of the strong medium heterogeneity. At the intermediate scale (~100 m), the determination of the hydrogeological karst properties can be studied by geophysical experiments. Therefore, a collection of geophysical observations at intermediate scale can be valuable to constrain numerical models and improve our understanding of epikarst processes. Various geophysical tools are used to monitor, at an intermediate scale, transfer and storage properties such as Magnetic Resonance Sounding (MRS) (Legchenko et al. 2002), 4D seismic (Wu et al., 2006; Valois, 2011), Electrical Resistivity Tomography (ERT) (Valois, 2011) and gravity measurements (Van Camp et al., 2006a; Jacob et al., 2010; Van Camp et al., 2017) among others. Both distributed geophysical measurements (ERT, 4D seismic) and integrative methods (MRS, gravity) revealed spatial variations associated to mid-scale heterogeneities.

Gravity methods are nowadays pertinent tools for hydrogeological studies in various contexts (Van Camp et al., 2006a; Davis et al., 2008). The value of the gravity at Earth surface is indeed directly influenced by underground rock density. A variation of density due to water saturation at depth can be directly measured from the surface through the temporal variation of the gravity (Harnisch & Harnisch, 2006; Van Camp et al., 2006b). Modern and accurate ground-based gravimeters provide a direct measurement of the temporal water storage changes in the underground without the need of any complementary petrophysic relationship (Davis et al., 2008; Jacob et al., 2008; Jacob et al., 2010; Deville et al., 2012; Fores et al., 2017). Time-lapse gravity measurements stand as an efficient hydrological tool for the estimation of water storage variations in both saturated and unsaturated zone. Moreover, the sampling volume of the gravity is increasing with depth: at 10 meters depth, the gravity integrates over a surface of a circular area with a radius of about 100 m. Small scale heterogeneities are averaged in gravity observations. Processes identification and modeling of heterogeneous hydro-sytems require non-local observations. As surface gravity measurement integrates all density changes below the gravimeter, observed temporal variations can be related to both saturated and unsaturated zones. However, time-lapse surface gravity measurements alone provide poor information on the vertical water distribution. To remedy to the absence of vertical resolution, gravity measurements can be done at different depths in caves or tunnels (Jacob et al., 2009, Tanaka et al., 2011). Time-lapse Surface to Depth (S2D) gravity measurements allow estimating water storage variations in the unsaturated zone of the karst. Furthermore, S2D gravity experiments allow also more precise measurements by common mode rejection. Previous studies of gravity S2D measurements made in natural cave suggest that water storage variations in the epikarst can be a major part of total water storage changes across the aquifer (Jacob et al., 2009, Fores et al., 2017). In the present study, we use gravity data to quantify the influence of the epikarst in term of seasonal water storage in two karst systems in the south of France (SEOU and BESS in figure 1). We first present the hydrogeological situation of the sites and the experimental setup. Then the gravity data processing is detailed and results are presented. Results from another close-by site (Jacob et al., 2009) are reminded and discussed in comparison with the results from our additional site surveys (BEAU in figure 1). Subsequently, time-lapse S2D gravity variations are analyzed in the light of these depth distributions and of a complementary MRS sounding. Finally, the seasonal water storage for all sites is discussed in terms of processes during the recharge of the karst and its link with lithology and geomorphology.

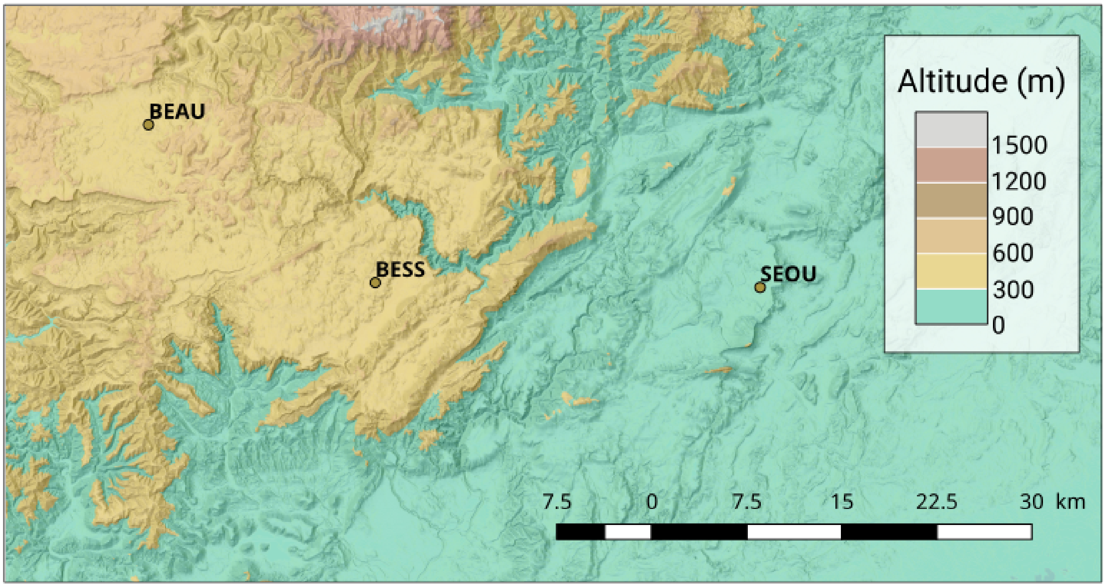

Figure 1: Topographic map (elevation in meters) with the three sites indicated

1) Hydrogeological setting of studied karst systems

In this study, measurements are reported for 3 sites in Southern France. The topographical situation of the study sites is shown in Figure 1.

a) Lamalou karst system (SEOU site)

The Lamalou karst system is located on the Hortus plateau (South of France). The aquifer is set in the 100 m thick formation of lower Cretaceous compact limestone (Fig. 2) deposited on Berriasian marls. These marls act as an impermeable barrier and define the lower limits of the saturated zone. Tertiary deposits overhang Cretaceous formations at the south-west and limit the aquifer. The karstified limestone formation is weakly folded as a NE-SW synclinal structure linked to the Pyrenean compression. The main recharge of the Lamalou karst system comes from rainfall which annually reaches 900 mm. Snow occurs less than once a year and is negligible in the seasonal water cycle. Surface runoff is extremely rare except during high precipitation events when most of the system is saturated (Boinet, 1999). Discharge of the Lamalou karst system only occurs at perennial Lamalou-Crès springs system composed of two perennial springs connected during high flow period (Durand, 1992). Daily discharge is 5 l/s and 1.5 l/s respectively for Lamalou spring and Crès spring (Chevalier, 1988). From combination of geomorphological observations, tracing experiments and mass balance modeling, the Lamalou recharge area is estimated to ~30 km² (Bonnet et al., 1980; Chevalier, 1988). The vadose zone has a maximum thickness of ~45 m. The epikarst thickness is estimated to 10 – 12 m depth at spring vicinity (Al-fares et al., 2002) and corresponds to an altered limestone with a strong secondary porosity such as opened fractures. Low matrix porosity has been estimated from core samples between 0.5 and 1.3%.

The Lamalou experimental site is a cave called Seoubio (SEOU) located to the North-East part of the system in Valanginian limestone (Fig. 2). The surface topography is nearly flat around the cave entrance, which corresponds to a vertical pothole of 5 m diameter and 30 m depth allowing a straight descent through the epikarst (Fig. 4a). The depth of the saturated zone is around 40 m below surface as attested by two siphons. The neighboring landscape is made of a 'lapiaz' structure with opened fractures and a thin soil. The land use around the site is a natural typical Mediterranean scrubland.

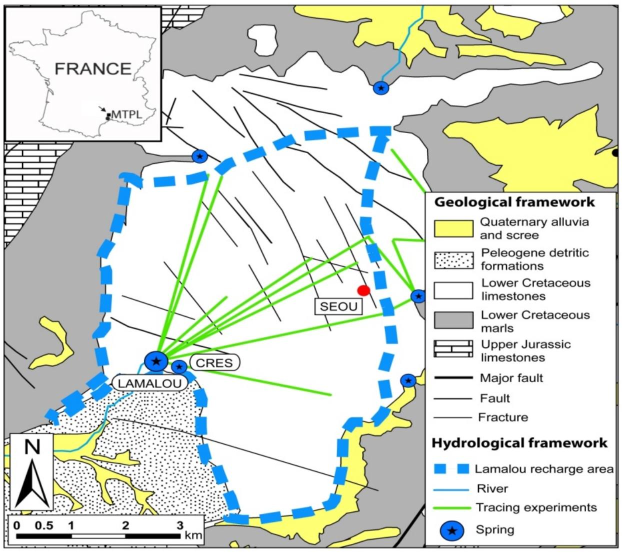

Figure 2: Hydrogeological setting of Lamalou karst system on the Hortus plateau. Seoubio cave (SEOU) is indicated by a red dot; MTPL shows the location of Montpellier city as a landmark.

b) Gourneyras karst system (BESS site)

The Gourneyras karst system is located in the southern part of Grands Causses area (south of France). The aquifer is set in Middle to Upper Jurassic limestone and dolomite topping Liassic marls formation. The latter formation defines the lower limit of the saturated zone of the karst system. The main recharge of the system comes from rainfall which reaches ~1100 mm annually. The rare snowfalls are included in the precipitation measurements. Discharge occurs only at the Gourneyras Vauclusian-type perennial spring. Discharge is not continuously monitored but punctual measurements suggest a discharge of ~20 m^3/s during flood events. Recharge area of Gourneyras spring is estimated to ~41 km^2 (SIE Rhône-Méditerranée, 2011).

The vadose zone has a maximum thickness of 450 m. Calcite filled fractures can be seen in the cave.

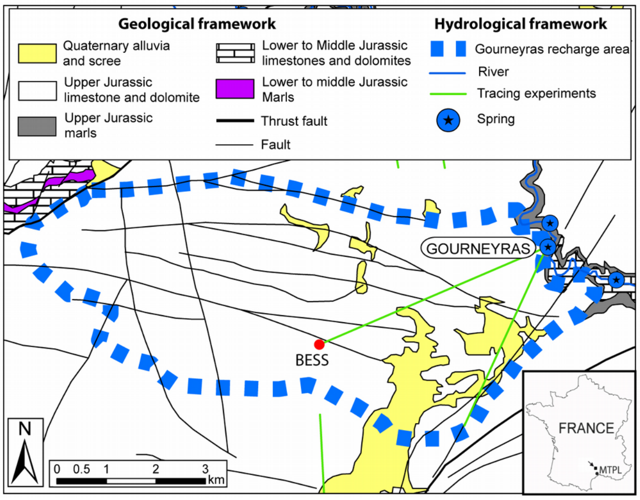

Figure 3: Hydrogeological location map of Gourneyras karst system. Besses cave is indicated by a red dot (BESS)

The Gourneyras experimental site is a cave called "Les Besses" (BESS) (Fig. 3). The surface topography around the cave entrance is a gentle slope to the south-east. The cave is located in Kimmeridgian limestone formations. At the cave location, limestones are covered by a thin dolomite formation. Typical porosity of the matrix from core samples ranges between 1.6 and 7% depending on the depth. Shallow alteration deposits such as clay are present at the surface. Above the cave, the land use is a natural typical Mediterranean scrubland. The cave morphology allows an easy afoot descent except between 670 m and 690 m elevation where abseiling rope is necessary. The cave topography allowed to perform gravity measurements at 5 different depths (Fig. 4b). Saturated zone is probably at 450 m depth below the surface, a few tenths of meters above spring elevation.

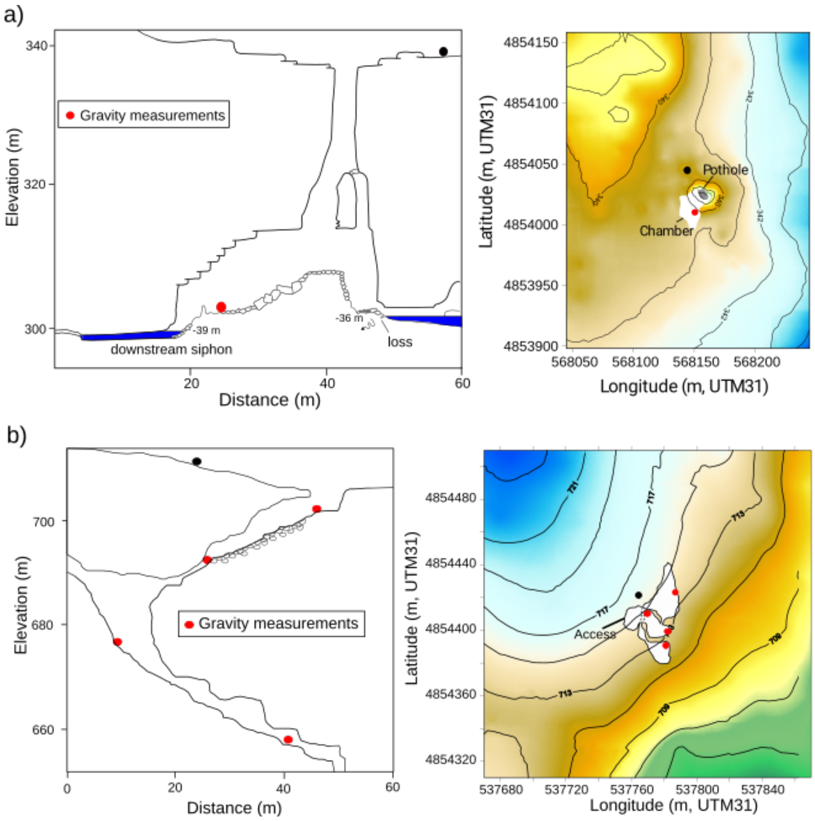

Figure 4: Developed cross-section and topography surrounding a) Seoubio caves, after Boinet (2002); and b) Besses caves. Black and red circles indicate the location of gravity measurements. Elevations are in meters. The projections of the cave in surface are represented in gray on topography.

The two karst systems of SEOU and BESS sites have been presented above but the results from a previous study (Jacob et al., 2009) are extensively used in the discussion (BEAU site). A detailed description of the site BEAU is available in Jacob et al. (2009). BEAU and BESS sites are located 25 km away at the same elevation with a similar geological and climatic setting. However, the BEAU site is embedded in a highly altered dolomite (typical porosity from core sample between 5 and 11%) capped with a shallow soil of the Durzon karst hydro-system.

2) Data acquisition and processing

a) Cave topography

Positions of cave gravity stations at each site were measured using standard speleologists tools. Azimuth, inclination and distance measurements were performed along 2 topographic surveys between surface and depth stations. The closing misfit between these surveys indicates an elevation accuracy of about 0.2 m.

b) Meteorological data

Precipitation and potential evapotranspiration are provided by the French national meteorological agency (Météo-France). The nearest meteorological station of each site was selected. Precipitations are daily monitored respectively at 4 km to the South-East of SEOU site and 5 km to the South of BESS site. Rain gauges are automatic tipping-bucket with a resolution of 0.2 mm. Accuracy of rain gauges is equal to 4% during weak precipitation, but the errors increase when precipitation exceeds 150 mm/h (10% accuracy) (Civiate & Mandel, 2008), which is rare in the area. The rainfalls are spatially homogeneous at the seasonal scale but not at the event scale (Fores et al., 2017). Both sites (BESS and SEOU) are mainly influenced by Mediterranean climate even if in BESS a clearer influence of the oceanic climate can be observed. Daily potential evapotranspiration (PET_d) is calculated using Pennman-Monteith's formula by Météo-France. PET_d is given at respectively 7 km to the south-west of SEOU site and 5 km to the south of BESS site. The actual evapotranspiration *(AET)* was calculated from the potential evapotranspiration (PET_d) and a crop coefficient (k). The crop coefficient is time-variable (i.e. during a season) (Allen et al., 1998) and includes effects of water availability and physiological properties of plants. The seasonal variation of the crop coefficient has been evaluated from 2 years of direct monitoring of actual evapotranspiration by a flux tower (Fores et al., 2017) and daily potential evapotranspiration (PET_d). The crop coefficient varies seasonally between 0,55 in summer (as low soil moisture is available) and 1,20 in winter. The same crop coefficient has been used on the three sites as the climate and the land use are similar. On an annual baseline, the average crop coefficient ranges between 0,5 and 0,7 in the same area (Jacob et al., 2009).

Due to the lack of realistic error estimation, accuracy of AET is fixed to 15% based on recent estimation of AET from flux tower measurements (Fores et al., 2017). As the ratio AET versus precipitation amount is much smaller during winter than during summer, the impact of the AET uncertainty is higher during the discharge period (summer) and allows more confident interpretation during the recharge period (winter).

c) MRS survey

At the site BESS, two MRS survey has been conducted in May 2011 and Aug. 2011. A NUMIS-LITE equipment from IRIS Instruments has been used with a 40×40 m square loop. A notch filter is used for cutting the harmonics of 50 Hz. The data were processed and inverted with SAMOVAR-11.3 software (Legchenko et al., 2004) using the procedure detailed in Mazzilli et al. (2016).

d) Surface to depth gravity experiment

Experimental setup

The surface to depth (S2D) gravity experiment consists in measuring the time-lapse gravity difference between surface and depth at a given site. The morphology of the caves allows measurements inside the karst and at different depths in the unsaturated zone. For each karst system we choose one cave where the surface and the underground access can be managed with a relative gravimeter. S2D gravity measurements are done at the surface and ~-35m depth at the SEOU cave. For BESS cave, gravity stations are located throughout the cave at different depths: the surface, -12 m, -23 m, -41m and -53 m.

The gravity measurements encompass a time span of 1.5 year from 02/2010 to 09/2011. Gravity was measured in late summer and early spring in order to evidence the seasonal water cycle. When more than two measurements per year have been done, all the results are averaged at a bi-annual frequency.

A relative gravimeter (Scintrex CG5) was used to measure the relative difference in gravity between two locations or stations. Scintrex relative gravimeters CG5 were used for precise micro-gravity survey (Bonvalot et al., 2008; Merlet et al., 2008; Jacob et al., 2010; Pfeffer et al., 2013). The gravity sensor is based on a capacitive transducer electrostatic feedback system to counteract displacements of a proof mass attached to a fused quartz spring. The CG5 instrument has a reading resolution of 1 µGal and a repeatability smaller than 10 µGal (Scintrex limited, 2006). The compactness and the precision of the gravimeter match the requirements of micro-gravity in natural caves. As gravity signals of hydrological processes display relatively small variations of 10-30 μgal, a careful survey strategy and processing must be applied to gravity data. To limit temporal bias linked to gravimeter position, the height and orientation of the CG5 gravity sensor are fixed for all stations using a brass ring positioned on drilled holes in the bedrock. We used only the CG5#167 for the measurements because of its known low drift and to limit instrumental biases.

Gravity data processing and error estimation

As demonstrated by Budetta and Carbonne (1997), Scintrex relative gravimeters need to be regularly calibrated when used to detect small gravity variations over extended periods of time. The calibration factor was measured before each gravity period at the Montpellier-Aigoual calibration line (Jacob, 2009). The accuracy of the calibration is 10^{-4}. Calibration factor of CG5#167 had not significant variations during the studied period (appendix 1).

The gravity data are corrected for Earth tides using ETGTAB software (Wenzel, 1996) with the Tamura tidal potential development (Tamura, 1987). Considering the distance of Atlantic Ocean, the ocean loading effects are weak (6 µGal) and have been removed using Schwiderski tide model (Schwiderski, 1980). Atmospheric pressure loading is corrected using a classical empirical admittance value of -0.3 µGal/hPa (pressure measurements have an

accuracy of about 1 hPa with a field barometer). Polar motion effects are not corrected because they are nearly constant over the time span of one gravity survey (~ 8 hours).
The drift of the CG5 sensor is linked to a creep of the quartz spring and must be corrected to obtain reliable values of gravity variations. To estimate the drift, gravity surveys are setup in loops: starting and ending at the same reference station. The reference station is occupied several times during a survey. The instrumental drift is assumed to be linear during the short time span of the loops (less than one day). The drift of the CG5#167 gravimeter is known to be particularly small around 100 µGal/day (Jacob et al., 2010). The gravity differences relative to the reference station and the drift value are obtained using a least-square adjustment scheme with the software MCGRAVI (Belin, 2006) based on the inversion scheme of GRAVNET (Hwang et al., 2002). Parameters to be estimated are gravity value at each station (surface and depths) and the linear drift of the gravimeter. Measurements of one station (m_d) relative to the reference station (m_s) can be expressed as:

$$C_f\left(m_s^{t_j}-m_d^{t_i}\right)+v_{S_i}^{S_j}=g_s-g_d+D_k\left(t_j-t_i\right) \qquad (1)$$

Where C_f is the calibration correction factor, m_s^{tj} and m_d^{ti} respectively the reference and station gravity reading at time t_j and t_i, v_{Si}^{Sj} the residuals of (m_s^{tj} - m_d^{ti}), D_k the linear drift of the loop k, g_s and g_d the gravity values at the reference and the station. The variance of one gravity reading is given by the standard deviation of 90 s measurements series and additional errors of 2 µGal for inaccurate gravity corrections and possible setup errors. The a-posteriori variance of unit weight is computed as:

$$\sigma_0^2=\frac{V^T PV}{n-(m+s)} \qquad (2)$$

Where n is the number of gravity readings averaged for each station occupation, s the number of loops, m the number of gravity station, V is an n vector of residuals and P is a weight matrix. The table in appendix 1 summarizes the results of the gravity experiments at each site. One can note that gravity errors budget is smaller than the measured gravity variations; this validates the survey setup and processing.

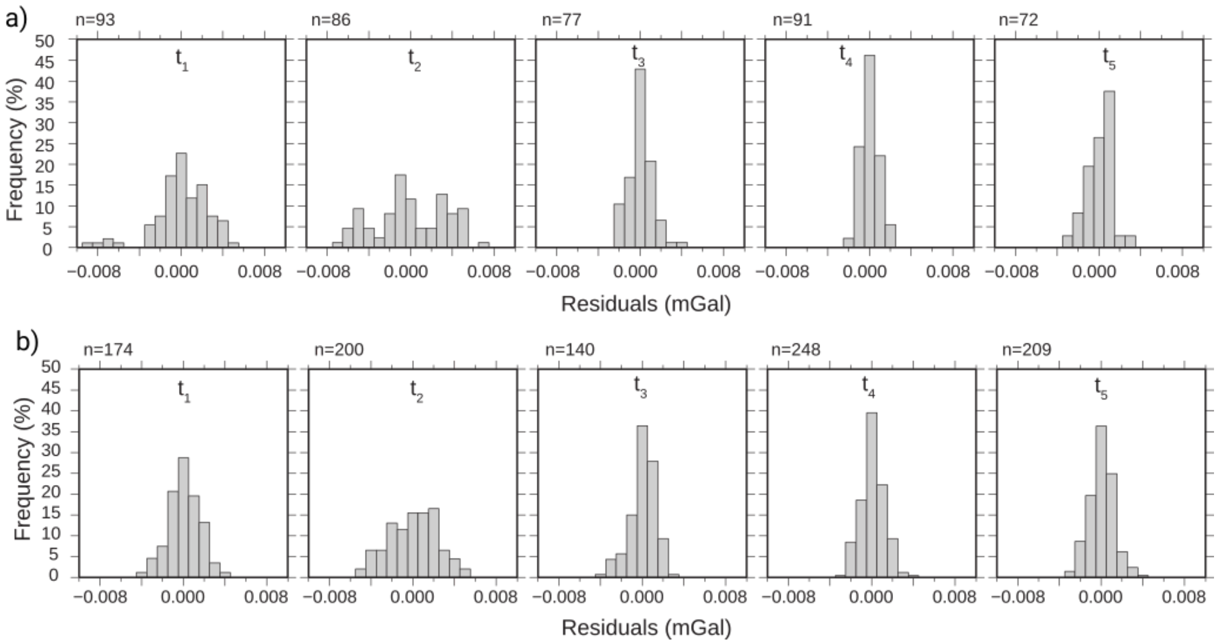

Figure 5: Histogram of residuals of the observed gravity differences versus the adjusted gravity differences at a) SEOU site, and b) BESS site for each measurements periods. During t1 and t2, short term strategy was used and long-term strategy during t3, t4, t5.

Measurement relaxation and measurement strategy

In addition to the daily drift, the transport of the gravimeter causes a relaxation of the quartz spring that leads to a rapid variation of the gravity value during the first ~40 minutes of measurements (in our case for the CG5 #167). This relaxation has already been described in previous studies such as Flury et al. (2007). The relaxation may sometimes be greater than the drift of the gravimeter and displays variable amplitude depending probably on the time and the type of transport and meteorological variations. Contrary to the drift, reasons of the relaxation are not clearly understood and cannot be modeled. Without the correction of the relaxation, the relative gravity measurements must be accounted for in the error budget. To resolve this problem, we setup a new measurement strategy which allowed removing relaxation and we compare it with a usual gravity measurements strategy.

Two measurement strategies are used in this study. The usual one, called “short time strategy” consists to multiply the occupations at all the stations (4 and 5 loops in our case). For each single occupation, 10 measurements of 90 s at 6 Hz sampling are performed. Only the last 5 or 6 nearly constant measurements are selected. Frequent reference station measurements during a loop allow for constraining the instrumental drift and the number of occupations leads to a statistical decrease of the error. With the short time strategy, one assumes that the relaxation due to the transport always results to the same bias from site to site. The time of

transportation between two stations is kept as constant as possible to obtain similar relaxation bias. This strategy was used for the two first gravity surveys (winter 2010 and summer 2010). The new strategy, called “long time strategy” aims to overcome the relaxation phenomena and was used for the three last gravity surveys. Only two or three occupations at the reference station and only one at the other stations are done. For each occupation, a minimum of 40 measurements of 90 seconds at 6 Hz sampling are performed (~ 1 hour). The rather large occupation time is necessary to ensure that the instrument has relaxed. The gravity reading then follows the daily linear drift. A minimum of 20 gravity readings during the linear, stable measurement period are kept. This strategy can be applied only if the non linear part of the drift is small, which is the case for CG5#167 gravimeter.
The evaluation of the measurement precision can be partially done with the help of the residuals. The residuals are the differences between the measured gravity value and the estimated gravity value. The residuals depend on the precision of the processed data and on the robustness of measurements strategy. For example, if a histogram of residual is centered on 0, it suggests that the correction processes have not introduced a bias in the gravity value estimation. The dispersion of the residuals can indicate noisy measurements or non-linear drift. The shape of the histogram shows the global precision of dataset. The residuals were estimated for each dataset (Fig. 5) and can be used to compare the two measurement strategies.

Most of the histograms display a Gaussian shape centered on zero with a small dispersion showing the good quality of the gravity readings and hence the robustness of the surface to depth gravity differences (Δg_{S2D}). However, the residuals of -8 µGal (Fig. 5a) for the period t_1 at SEOU site are due to an unexpected gravity jump during the survey. As no explanation was found for the gravity jump, they are kept for data adjustment even if the dispersion of the gravity residuals increases accordingly. For the two first datasets, 90 % of residuals are comprised in 8 µGal intervals. For the three last datasets, 90 % of residuals are between -2 µGal and +2 µGal. Residuals histograms of the “long time strategy” are narrower than those of the “short time strategy” which confirms the improvement of the field experiment strategy (Fig. 5). The relaxation due to transportation or non-linear drift would have induced non Gaussian shape of the histograms and not centered on zero as seen during the survey 2 at SEOU site (Fig. 5a). We have tested in a cave the “long time strategy” using repeated measurement on a single station interrupted by hand transportation. As for the data shown here, these unpublished results, show a smaller dispersion of the residuals than the one provided by the “short time” method and an unbiased mean.

Gravity data after correction and drift adjustment are presented in the appendix 1. For SEOU site, the Δg_{S2D} values show significant temporal variations ranging from -3.897 mGal to -3.914

mGal. At BESS site, between surface to 12 m depth, Δg_{S2D} values is ranging from -1.523 mGal to -1.537 mGal. Below 12 m, gravity variations are not significant.

3) Data interpretation

Surface to Depth formulation

The ***ΔgS2D*** gravity values contain the variations associated to elevation and to the differential attraction of rocks masses. These time independent effects must be removed for accessing to water storage variations. In the following we assume that the sedimentary formations between the two measurement sites have no lateral variations of density.

Once surface to depth gravity differences are calculated, looking at temporal variations allows for retrieving the water storage variations. Time-lapse S2D gravity can be interpreted in term of equivalent water height changes, assuming that the water storage variations are laterally homogeneous at investigated temporal (seasonal) and spatial (~100 m) scales. Such hypothesis is likely to be untrue in a karstic area because of voids and heterogeneities potentially present at all scales. Looking at a temporal snapshot of the total water storage (porosity times saturation) in the first meters of the karst should probably show a high heterogeneity as seen in boreholes. Nevertheless, we justify our working hypothesis as follows:

- ✓ S2D gravity measures at an *intermediate (100 m) scale*. The laterally integrative property of the gravity leads to ignore small scale (up to a few meters) heterogeneities which is one of the main advantage of the gravity method. The large scale heterogeneities (> 100 m) are negligible as they have an equivalent impact on the gravity measurements in surface and in depth (common mode rejection in the S2D method).
- ✓ Time-lapse S2D gravity measures underground water variations associated to a *seasonal water cycle*. At the seasonal time-scale, the storage function of the karst is probably largely dominant and the fast transfer (at the flood scale) is not measured.
- ✓ Time-lapse S2D gravity measures the average water storage *variations* (i.e. porosity times saturation variations). As in our case the epikarst is never completely saturated during the measurements, the heterogeneity of the water storage variations is likely to be associated to saturation variation (due to climate) and not to porosity (due to heterogeneities).

For the duration of investigation, the effects of erosion on topography, caves and potential tectonic activity can be considered as negligible for all sites. Additionally, temporal variations of the terrain correction are not significant (Jacob et al., 2009). Hence, the evolution of surface to depth gravity with time can be reduced to:

$$\Delta_z^t g = 4\pi G \Delta_z^{\delta t} \rho_{app} h \qquad (3)$$

Where $\Delta^t\rho_{app}$ is the apparent density change over time t. Surface to depth gravity variations during time period $\Delta_z^t g$ correspond to twice the Bouguer attraction of a plate with $\Delta^t\rho_{app}$ density of height h and increases by two the signal to noise ratio. Finally, the apparent density variations depend only on water saturation variations. Time-lapse water saturation variation can be approximated to an equivalent water height (EqW) variation $\Delta^t_z l$, then equation (3) becomes:

$$\Delta_z^t g = 4\pi G \rho_w \Delta_z^t l \qquad (4)$$

where ρ_w is water density. Therefore, a S2D gravity difference of 2 μGal is associated to an effective water slab of 23.86 mm.

Site	*Time period*	*Gravity difference (μGal)*	*EqW Equiv. Water height (mm)*	*Cumulative precipitation (mm)*	*Cumulative AET (mm)*	*NWI Net water inflow (mm)*	*EqW / NWI ratio (%)*
SEOU	Feb10-Aug10	-17 ± 3.9	-203 ± 48	281 ± 11	377 ± 56	-96 ± 58	212
	Aug10-May11	8 ± 3.9	95 ± 48	628 ± 25	328 ± 49	300 ± 55	31
	May11-Sep11	-3 ± 2.0	-35 ± 25	256 ± 10	309 ± 46	-53 ± 47	67
BESS (0-12m)	Feb10-Aug10	-14 ± 3.1	-167 ± 37	315 ± 13	473 ± 71	-158 ± 72	105
	Aug10-May11	9 ± 3.5	107 ± 42	854 ± 34	471 ± 71	383 ± 78	28
	May11-Sep11	-9 ± 2.6	-107 ± 31	162 ± 6	441 ± 66	-278± 66	38
BEAU	Sep06-Nov06	26 ± 2.5	310 ± 30	445 ± 18	70 ± 10	375 ± 21	83
	Nov06-Sep07	-20 ± 3.2	-238 ± 38	482 ± 19	502 ± 75	-20 ± 78	*
	Sep07-Feb08	25.8 ± 3.0	307 ± 32	424 ± 17	201 ± 30	223 ± 34	137

Table 1: Time-lapse S2D gravity difference, Equivalent water height, cumulative precipitation, cumulative actual evapo-transpiration and total water inflow with the associated errors at SEOU, BESS and BEAU site for different recharge and discharge periods. Recharge periods are indicated by the gray color. For BEAU site, only measurements with the CG5 #167 are kept.

The measurements must be done during the minimum and maximum of the seasonal water cycle: the seasonal cycle is measured with a minimum uncertainty and the potential aliasing is reduced. In the Mediterranean climate, high precipitation events (HPE) have a large impact in the yearly accumulated precipitations. HPE occurs mainly in autumn, especially in September.

In 2011 an exceptional HPE occurs in March: an additional gravity survey (t4) was done in early May 2011 to reach the complete recharge. The low temporal sampling of the gravity survey could produce aliasing. To limit the impact of the aliasing, gravity surveys (except at SEOU site in Feb. 2010) were not planned just after significant rainfall events. The absolute gravity monitoring done in the Larzac near BESS site (Deville et al., 2012) were used to monitor the recharge, to adapt the S2D gravity surveys dates and to reduce the potential aliasing.

During all discharge periods, gravity differences are negative in the three sites indicating a decrease of EqW. For all recharge periods, gravity differences are always positive indicating an increase of EqW. At SEOU site, the two dry seasons lead to a loss of about 203 mm and 35 mm EqW respectively for first and second discharge period. During recharge period, increase of EqW is equal to 95 mm, in accordance with high precipitation value during this period. At BESS site between 0 and 12 m, the two discharge periods show a similar loss around 167 mm and 107 mm. Recharge period has a positive EqW equal to 107 mm with the respect of high precipitation value. At BEAU site, only one discharge period was monitored and the loss is equal to 238 mm. For the two recharge periods EqW have the same value around 300 mm, larger than SEOU and BESS sites. Except for the first recharge period at the SEOU site, the EqW during recharge and during discharge are equivalent.

Seasonal water storage

As the precipitation and the evapotranspiration can vary geographically from site to site, EqW cannot be directly compared. Looking to the ratio between the time-lapse S2D gravity variations (or EqW) and the net water inflow (NWI) allows the inter-comparison between different sites and the interpretation in terms of water storage capacities. The normalization of EqW by the net water inflow allows also comparing EqW measured at other time period, for example at BEAU site in 2007-2008. As no surface runoff has been observed at the three sites, we consider that all rainfall directly infiltrate into the soil. As AET contributes to remove water from the soil, it was taken into account in the mass balance. The effective precipitation or the net water inflow during a time period is the difference between the cumulative precipitation (P_c) and the cumulative actual evapotranspiration (AET_c) for the given site:

$$NWI = P_c - AET_c \qquad (5)$$

The net water inflow exhibits as expected a seasonal cycle. High values (up to 383 mm) during the recharge and small or negative value during the discharge (down to -278 mm) were estimated (Table 1).

During the discharge period, EqW and NWI are all negative. The EqW is larger (in absolute value) than NWI for the February 2010 to August 2010 discharge period at SEOU and BESS site. On the opposite, for May 2011 to September 2011 discharge period, EqW is lower (in absolute value) than NWI (Table 1). Such unrelated relationship between EqW variations and NWI seems to be typical of the discharge and prevent simple interpretation. The discharge is also characterized by a high error budget of NWI value as the evaluation of AET is dependent of the relative low accuracy of the crop coefficient. As during the discharge the AET is important compared to the precipitations, the uncertainty of AET prevents further interpretation. The discharge period is therefore not included in the following discussion.

During the recharge, the two sites BESS and SEOU exhibit a similar pattern as the EqW is smaller (about 30%) than the net water inflow (Fig. 6). For example, at BESS site EqW is equal to 107 mm when the net water inflow reaches 383 mm. On other hand, during the same season, EqW and NWI are similar at BEAU site (83 and 137 %). As the EqW/NWI ratio is a climatic normalization, the heterogeneity in the seasonal water storage is therefore clearly shown as expected in a karstic environment. The EqW/NWI ratio confirms the direct S2D measurements reading with larger S2D gravity variations at BEAU than at SEOU and BESS (Fig. 6).

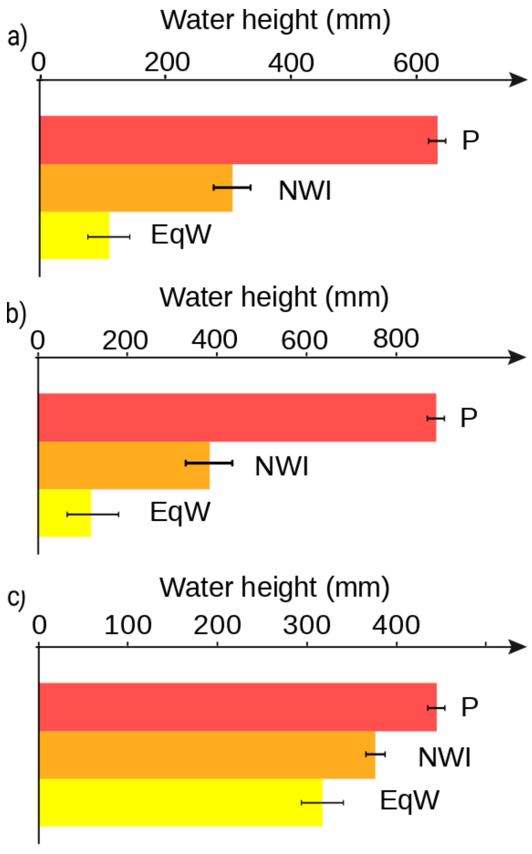

Figure 6: Precipitation, net water inflow and EqW during recharge period for a) SEOU site; b) BESS site and c) BEAU site.

Depth distribution of seasonal EqW

Results summarized in Table 1 for BESS site are the EqW between the surface and the 12 m depth station. In the BESS site, EqW deduced from gravity measurements are available at 5 different depths. Gravity depth profiles have nearly the opposite shape during recharge and discharge periods (Fig. 7). During recharge period, gravity variation is equal to 107 mm (9 µGal) between surface and 12 m depth with a small error budget (3 µGal). Below 12 m depth, gravity variations are not significant (< 3 µGal for the second, the third and the fourth depth stations). For the second discharge period, time-lapse S2D gravity variation has also a value of 107 mm (-9 µGal) for the first depth with 2.5 µGal of error budget with not significant gravity variations below.

The vertical gravity profile can be compared to the MRS vertical profiles at the same place (Fig. 7). The MRS profile clearly indicate a significant water content near the surface with a maximum around 10 m depth. The correlation between the both independent geophysical methods confirm the importance of a superficial reservoir in the first 10 m depth. No significant variations between the two MRS survey can be evidenced from the inversions. It allow to quantify a maximum MRS water content variations around 1 % (130 mm in EqW) in the first 10 m depth. The 1 % maximum MRS water content variations is coherent with the gravity estimation around 100 mm.

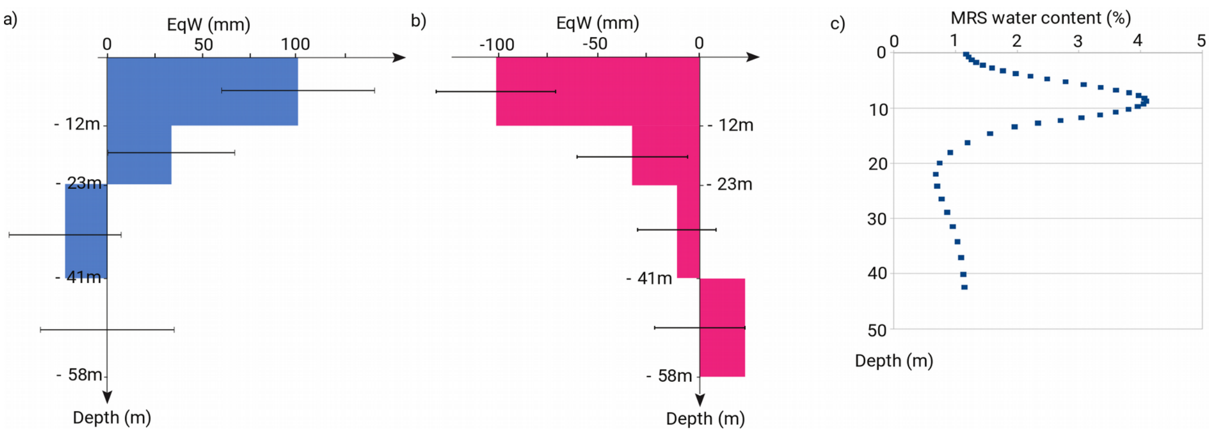

Figure 7: S2D gravity difference function of depth at the BESS site for a) recharge period (t2-t4) in 2010; b) and discharge period (t4-t5) in 2011; c) MRS profile of May 2011 at the BESS site.

4) **Discussion**

Precision of S2D measurements

We show using two measurement strategies that the error budget can be minimized. A long time measurements strategy (45 min per site) displays a better error budget than a short time strategy (10 min per site). However, we perform the long time strategy with a unique measurement on each station (except the base station). This strategy can be performed only if the gravimeter has a quasi-linear drift. For the site BESS, the similarity of the gravity measurements with the MRS profile (Fig. 7) is an indirect information of the quality of the gravity measurement. The coherence of the gravity between the wet and the dry season is another indirect confirmation of a significant signal to noise ratio. From the MRS, the water content variations should not vary significantly below 15 m. The S2D gravity below 15 m depth ranges between -3 and 3 µGal, leading to another estimation of the S2 gravity precision around 3 µGal. The measurements are suitable for a quantitative interpretation of differential gravity in term of water storage.

Quantification of the epikarst water storage

The gravity survey done at BESS site allow evaluating the depth distribution of the seasonal water storage variations. Both recharge and discharge periods show water storage variations in unsaturated zone located within the first 12 meters (Fig. 7), with a seasonal water storage of up to 107 mm (9 µGal). The water content between 12 m and 58 m depth is too small to be measured by both the gravity and the MRS. At BESS site, the subsurface reservoir can be identified as the surface thin dolomite formation and/or as an epikarst, both being characterized by an enhanced porosity. Various studies support the hypothesis of a key role of the epikarst in the seasonal water storage (Mangin, 1975; Perrin et al., 2003; Klimchouk, 2004; Williams, 2008). Weathered structures (and especially in dolomite rocks) allow water reservoir in the first few meters of the unsaturated zone of karst system. Following Williams (2008), epikarst thickness may vary from zero to 30 m and epikarst water storage occurs because of a strong porosity in the epikarst associated to a reduced permeability at its base. Surface to depth gravity and MRS allows at BESS site a precise quantification of both thickness and amplitude of subsurface water storage.

The knowledge of the amount and depth of water storage in epikarst provide new and quantitative information for the modeling of groundwater transfer. The epikarst reservoir is a major parameter for pollution vulnerability mapping in karst hydrosystem as in the PaPRIKa (Protection of the aquifers from the assessment of four criteria: Protection, Rock type, Infiltration and Karstification degree) for example (Dorfliger et al., 2010). Pollution can reach the spring in a few days (fast transfer), but another part of the pollution can be stored seasonally in the epikarst. In particular, high water content in subsurface may facilitate the piston flow effect and accelerate the flood dynamics but not necessary the transport. The coupling between gravimetric hydrological and MRS measurements may provide significant knowledge on unsaturated aquifer vulnerability to pollution: Mazzilli and co-authors (2016) highlight the role of water saturation in the infiltration zone from MRS survey mapping in nearby Larzac karst area.

Variability of epikarst water storage

Comparison of the ratio EqW versus NWI allows a quantification of the transient water storage in the epikarst. Significant seasonal water storage is measured at the three sites but different associated ratio. Overall, the results confirm the role of the epikarst as an active reservoir at seasonal time scale but also highlight the heterogeneity of the karst. During recharge period, EqW increase correspond to 30 % of NWI at SEOU and BESS sites whereas at BEAU site EqW increase is as large as 80 % of NWI.

The variability of the ratio EqW versus NWI can be associated to a variety of factors: lithology, thickness of the unsaturated zone or depth of the measurements, thickness of the epikarst, intensity of the fracture and alteration, among others. The thickness of unsaturated zone could be correlated with its storage capacity if the storage was occuring on the whole thickness. Regarding the three sites, BESS and SEOU site have a similar EqW to NWI ratio in spite of a large difference of unsaturated thickness, which are respectively of 40 m and 300 m. Also, BEAU and BESS site have a similar unsaturated thickness (200-300 m) but have a great difference in EqW to NWI ratio. Our case suggests that the thickness of unsaturated zone is not a critical factor influencing seasonal water storage capacity of the karst.

The EqW to NWI ratio from the gravity measurements is now interpreted in the terms of karst morphology or lithology. Water storage capacity in the three site is largely dependent on the kind of host rock: limestone for BESS (except a few meters in subsurface: dolomite) and SEOU sites and dolomite for BEAU site.

A high ratio of the NWI is stored in subsurface in the dolomite site BEAU as expected from others studies in the same area (Fores et al., 2017). The amount of gravity variations is typical of the area and significantly larger than BESS and SEOU sites. In the compact limestone sites (BESS and SEOU), only one third of the NWI is stored. Alteration of the dolomite develops new micro-porosity which in turn increases the reservoir properties (Quinif, 1999). Enlarged fractures associated to secondary porosity are also filled by the residuals of dolomite alteration (sand). By contrast, in BESS and SEOU sites the limestone is rather characterized by a low to medium micro-porosity (characterized by core samples porosity measurements from 0.5 to 5 %) drained by open fractures. Only a small part on the net water inflow can be stored in the primary and secondary porosity. As a consequence, seasonal water storage capabilities of dolomite are more important than those of limestone. Unsaturated zone of dolomite karst (BEAU site) has a large capacitive function (up to 80% of NWI) and a relatively limited transfer function. On the opposite, unsaturated zone of limestone karst system (SEOU and BESS sites) has a reduced capacitive function (around 30% of NWI).

Previous studies indicate that epikarst has a large capacitive function and corresponds to a main seasonal stock of water (Klimchouk, 2004; Williams, 2008). The predominant role of epikarst for water storage is confirmed by the S2D gravity survey and the MRS. However, porosity is highly dependent of the type of limestone and our two sites have compact limestone. The impact of the lithology should be further studied by adding different sites in the same hydro-climatic context with complementary measurements such as MRS and core samples (Mazzilli et al., 2016). From MRS mapping survey conducted by Mazzilli and co-authors (2016) in the nearby Larzac area, one important result is the high water content not only in the subsurface or epikarst but also in the infiltration zone, independently of the lithology. The BESS site water content profile is not typical but an exception. The main geological particularity of the BESS site is the thin top formation of dolomite above the limestone which could enhance the capacitive function of the epikarst.

Capacitive and transmissive reservoir properties

When surface only gravity time-series are associated to a simple hydrological model to correct surface effects (topography and building umbrella effect), reservoir transfer properties (hydraulic conductivity or specific yield) can be determined (Deville et al., 2012), but it requires continuous or frequent gravity measurements. Thus is not the case in the present study, however, due to time-lapse S2D measurements, it is possible to partially estimate reservoir transfer properties. As gravity measurements are repeated seasonally, the ratios EqW versus NWI indicate if the water time transfer is larger than 6 months (or not). During the recharge period, the epikarst reservoir is filled by water fluxes from surface. As large seasonal water storage is observed in BEAU, the transfer time of the epikarst reservoir should excess 6 months. On the other hand, almost no inter-annual cycle has been observed (Deville et al., 2012) for the Durzon karst system from surface absolute gravity measurements, therefore, the transfer time should be less than one year. The range of transfer time is also in accordance with the model result obtained for the Durzon karst system. An intermediate transfer time of the epikarst reservoir to the infiltration zone of about 6-12 months can be proposed for altered dolomite karst with a lack of high transmissive fractures. This characteristic transfer time is in accordance with the models fitted using continuous superconducting gravity data (Fores et al., 2017).

On the other hand, only a small part of the NWI is stored in the limestone epikarst (BESS, SEOU) after the recharge period. A short transfer time (< 6 months) in the limestone karst is therefore necessary and can be due to open fracture as observed in surface. The poorly capacitive epikarst at SEOU site is highlighted by nearby MRS measurements (near the spring 5 km away) measuring water content between 0 and 1,7 % (Vouillamoz et al., 2003). Chevalier (1988) has also shown with the analysis of the spring water during flood events that water transfer is fast between surface to spring (few days) and the major part of the net water inflow is retrieved a few days after the rain at the spring.

Using a reservoir modeling with a classical Maillet (1905) law, transfer times of 3.5 months for limestone sites (SEOU/BESS) and 13 months for dolomite site (BEAU) can be estimated. One can finally look at the SEOU recharge 2010 survey which has an abnormal high EqW increase (table 1). The measure was done only a few days (one day) after a heavy rainfall and a significant part of water from rainfall is probably still present in the unsaturated zone.

5) Conclusion and perspectives

The time-lapse S2D methodology uses in-situ measurements in karst caves during a seasonal climatic cycle. As large volumes are investigated by gravity, small scale heterogeneities (~ 10 m) are averaged. Gravimetry allows investigating heterogeneities at intermediate or meso-scale (~100 m) well suited to further assimilation in numerical models. The three sites display different morphologies and lithologies. In all cases, a significant seasonal water storage is always measured. No relation between seasonal water storage amplitude and morphology of karst system (i.e. unsaturated zone thickness) has been observed. By contrast, the seasonal water storage (EqW) versus net water inflow (NWI) ratio seems to be dependent from the lithology. Especially, the alteration of the dolomite tends to enhance storage properties of the epikarst. In our study, the dolomitic epikarsts have greater capacitive function than limestone epikarst. We highlighted a different capacitive function between the two sites located in limestone with respect to the one embedded in a dolomite environment.

The thickness of the epikarst was estimated in the BESS site thanks to gravity stations regularly spaced in depth. The seasonal water storage mostly occurs in the 12 first upper meters in accordance with MRS profile. The 12 m sub-surface reservoir can be identified as the high porosity zone of the epikarst and/or dolomite versus limestone changes. The limestone infiltration zone below 12 m is only transmissive without seasonal water storage.

The transmissive function of the epikarst can be partially estimated from the gravity water storage estimations. In this study, the transfer times of recharge water are longer in dolomites (> 6 months) than in limestones (< 6 months). The study of the karst transfer function cannot be done directly from surface gravity measurements and this is a clear advantage of the S2D setup. The addition of an absolute (or continuous) gravity monitoring at the surface would allow to estimate the water storage between the surface and the measurements at depth and also deeper, and could give constrain on the infiltration / saturated zone.

Since this study focuses only on three sites, the results should be compared with other measurements in various karst systems to analyze more rigorously the impact of the fracture, the alteration and the lithology. Moreover, gravity observations should be combined with in-situ flux such as seepage or geophysical measurements, for example Magnetic Resonance Sounding (MRS) or ERT (Mazzilli et al., 2016) in order to study the relation between groundwater storage (from MRS) and transient seasonal variations of the groundwater storage (from gravity). These collocated measurements should lead to a better knowledge of unsaturated zone properties and processes as demonstrated for the BESS site.

Acknowledgments:

The project is part of the HydroKarst G² project from 2009 to 2013 funded by the French Agence Nationale de la Recherche (ANR). Gravity surveys were part of the OSU OREME funded by the Institut de Recherche pour le Développement (IRD) and the Institut National des Sciences de l'Univers (INSU) and of SNO-SOERE H+ (INSU). The Scintrex CG5 relative gravimeter was loaned by the Gravity Mobile facility (GMOB) of RESIF-INSU. We would also like to acknowledge the owner of SEOU and M. Magne, owner of BESS for letting us access the caves and M. Boucher for her help with the MRS survey. The paper benefited from reviews by two anonymous reviewers,

Al-fares, W., M. Bakalowicz, R. Guérin & M. Dukhan, 2002. Analysis of the karst aquifer structure of the Lamalou area (Hérault, France) with ground penetrating radar. Journal of Applied Geophysics 51: 97-106.

Allen, G. A., L. S. Pereira, D. Raes & M. Smith, 1998. Crop evapotranspiration - Guidelines for computing crop water requirements. Rome, FAO-Food and Agriculture Organization of the United Nations.

Bakalowicz, M., 2005. Karst groundwater: a challenge for new resources. Hydrogeology Journal 13(1): 148-160.

Batiot, C., C. Emblanch & B. Blavoux, 2003. Carbone Organique Total (COT) et Magnésium (Mg2+) : deux traceurs complémentaires du temps de séjour dans l'aquifère karstique. C. R. Geoscience 335: 205-214.

Beilin, J., 2006. Apport de la gravimétrie absolue à la réalisation de la composante gravimétrique du Réseau Géodésique Français, Institut Géographique National.

Boinet, N., 1999. Exploitation de la fracturation d'un massif par la karstification : exemple de Causse de l'Hortus (Hérault, France). Geodinamica Acta 12(3-4): 237-247.

Boinet, N., 2002. Inventaire spéléologique du Causse de l'Hortus-Tome 4.

Bonnet, M., A. Lallemand-Barres, D. Thiery, H. Bonin & H. Paloc, 1980. Etude des mécanismes de l'alimentation d'un massif karstique à travers la zone non saturée. Application au massif de l'Hortus. S. g. N.-S. H. Rapport du BRGM.

Bonvalot, S., D. Remy, C. Deplus, M. Diament & G. Gabalda, 2008. Insights on the March 1998 eruption at Piton de la Fournaise volcano (La Reunion) from microgravity monitoring. Journal of Geophysical Research-Solid Earth 113(B5).

Budetta, G. & D. Carbone, 1997. Potential application of the Scintrex CG-3M gravimeter for monitoring volcanic activity; results of field trials on Mt. Etna, Sicily. Journal of Volcanology and Geothermal Research 76(3-4): pp. 199-214.

Chevalier, J., 1988. Hydrodynamique de la zone non saturée d'un aquifère karstique : Etude expérimentale. Site du Lamalou-Languedoc, Université Montpellier 2: 195p.

Civiate, M. & F. Mandel, 2008. La mesure de hauteurs de précipitations - Fiche descriptive sur les instruments de mesure météorologique -Version 1.0. Météo-France.

Davis, K., Y. Li & M. Batzle, 2008. Time-lapse gravity monitoring: A systematic 4D approach with application to aquifer storage and recovery. Geophysics 73(6).

Deville, S., T. Jacob, J. Chery & C. Champollion, 2012. On the impact of topography and building mask on time varying gravity due to local hydrology. Geophysical Journal International, 192(1), 82-93.,

Dörfliger, N., Plagnes, V., & Kavouri, K. (2010). PaPRIKa a multicriteria vulnerability method as a tool for sustainable management of karst aquifers Example of application on a test site in SW France. SUSTAINABILITY OF THE KARST ENVIRONMENT, 49.

Durand, V., 1992. Structure d'un massif karstique. Relations entre déformations et facteurs hydrométéorologiques, Causse de l'Hortus - sites des sources du Lamalou (Hérault), Université Montpellier II. PhD Thesis.

Emblanch, C., C. Zuppi, J. Mudry, B. Blavoux & C. Batiot, 2003. Carbon 13 of TDIC to quantify the role of the unsaturated zone: the example of the Vaucluse karst systems (Southeastern France). Journal of Hydrology 279(1-4): 262-274.

Fleury, P., M. Bakalowicz & M. Becker, 2007. Characterising a karst system with a submarine spring: the example of La Mortola (Italy). Comptes Rendus - Academie des sciences. Geoscience 339(6): pp. 407-417, doi:410.1016/j.crte.2007.1004.1004

Flury, J.; Peters, T.; Schmeer, M.; Timmen, L.; Wilmes, H.; Falk, R., 2007. Precision gravimetry in the new Zugspitze gravity meter calibration system; Proceedings of the 1st International Symposium of the International Gravity Field Service, Istanbul 2006, Harita Dergisi, Special Issue, Nr. 18, pp 401-406, ISSN 1300-5790, 2007

Fores, B., Champollion, C., Le Moigne, N., Bayer, R., Chéry, J. (2017). Assessing the precision of the iGrav superconducting gravimeter for hydrological models and karstic hydrological process identification. Geophysical Journal International. 208(1), 269-280.

Harnisch, G. & M. Harnisch, 2006. Hydrological influences in long gravimetric data series. Journal of Geodynamics 41: 276-287.

Hu, C., Y. Hao, T. J. Yeh, B. Pang & Z. Wu, 2008. Simulation of spring flows from a karst aquifer with an artificial neural network. Hydrological Processes 22: 596-604.

Hwang, C., C. G. Wang & L.-H. Lee, 2002. Adjustment of relative gravity measurements using weighted and datum-free constraints. Computers & Geosciences 28(9): pp. 1005-1015.

Jacob, T., 2009. Apport de la gravimétrie et de l'inclinométrie à l'hydrogéologie karstique. Geosciences Montpellier. Montpellier, Université des Sciences et Technologies.

Jacob, T., R. Bayer, J. Chery, H. Jourde, N. Le Moigne, J. P. Boy, J. Hinderer, B. Luck & P. Brunet, 2008. Absolute gravity monitoring of water storage variation in a karst aquifer on the Larzac plateau (Southern france). J.of Hydrology 359(1-2): 105-117, doi:110.1016/j.jhydrol.2008.1006.1020.

Jacob, T., R. Bayer, J. Chery & N. Le Moigne, 2010. Time-lapse microgravity surveys reveal water storage heterogeneity of a karst aquifer. Journal of Geophysical Research-Solid Earth 115.

Jacob, T., J. Chery, R. Bayer, N. Le Moigne, J. P. Boy, P. Vernant & F. Boudin, 2009. Time-lapse surface to depth gravity measurements on a karst system reveal the dominant role of the epikarst as a water storage entity. Geophys. J. International 177: 347-360 doi: 310.1111/j.1365-1246X.2009.04118.x.

Klimchouk, A., 2004. Towards defining, delimiting and classifying epikarst: Its origin, processes and variants of geomorphic evolution. Proc. of the symposium held October 1 through 4, 2003 Sheperdstown, West Virginia, USA. Karst Water Institute special publication, Epikarst 9(1): 23-25.

Lastennet, R. & J. Mudry, 1997. Role of karstification and rainfall in the behavior of a heterogeneous karst system. Environmental Geology 32(2): 114-123.

Legchenko, A., J. M. Baltassat, A. Beauce & J. Bernard, 2002. Nuclear magnetic resonance as a geophysical tool for hydrogeologists. Journal of Applied Geophysics(50): pp. 21-46.

Mangin, A., 1975. Contribution à l'étude hydrodynamique des aquifères karstiques, Université de Dijon. Ph.D. Thesis: 124.

Marin, A. I., N. Doerfliger & B. Andreo, 2012. Comparative application of two methods (COP and PaPRIKa) for groundwater vulnerability mapping in Mediterranean karst aquifers (France and Spain). Environmental Earth Sciences 65(8): 2407-2421.

Mazzilli, N., Boucher, M., Chalikakis, K., Legchenko, A., Jourde, H., & Champollion, C. 2016. Contribution of magnetic resonance soundings for characterizing water storage in the unsaturated zone of karst aquifers. Geophysics, 81(4), WB49-WB61.

Merlet, S., A. Kopaev, M. Diament, G. Geneves, A. Landragin & F. Pereira Dos Santos, 2008. Micro-gravity investigations for the LNE watt balance project. Metrologia 45: 265-274 doi: 210.1088/0026-1394/1045/1083/1002.

Perrin, J., P. Jeannin & F. Zwahlen, 2003. Epikarst storage in a karst aquifer: a conceptual model based on isotopic data, Milandre test site, Switzerland. Journal of Hydrology 279: 106-124.

Pfeffer, J., C. Champollion, G. Favreau, B. Cappelaere, J. Hinderer, M. Boucher, Y. Nazoumou, M. Oï, M. Mouyen, C. Henri, N. Le Moigne, S. Deroussi, J. Demarty, N. Boulain, N. Benarrosh, O. Robert, 2013. Evaluating surface and subsurface water storage variations at small time and space scales from relative gravity measurements in semiarid Niger, Water Resour. Res., 49, 3276–3291, doi:10.1002/wrcr.20235.

Pinault, J. L., V. Plagnes, L. Aquilina & M. Bakalowicz, 2001. Inverse modeling of the hydrological and the hydrochemical behavior of hydrosystems; characterization of karst system functioning. Water Resources Research 37: 2191-2204.

Quinif, Y., 1999. Fantômisation, cryptoaltération et altération sur roche nue, le triptyque de la karstification. Actes du colloque européen Karst-99: 159-164.

Réméniéras, G., 1986. L'hydrologie de l'ingénieur. Paris, EDF et Eyrolles ed.

Schwiderski, E. W., 1980. Ocean tides, II: A hydrodynamic interpolation model. Marine Geodesy 3: pp. 219-255.

Scintrex limited, 2006. CG5 Scintrex autograv system Operation Manual. Concord, Ontario, Scintrex Limited.

SIE Rhône-Méditerranée, e.-f. (2011). Fiche de caractérisation des masses d'eau souterraine : Calcaires et marnes Causses et avant-Causses du Larzac sud, Campestre, Blandas, Séranne,. from http://www.rhone-mediterranee.eaufrance.fr/.

Tamura, Y., 1987. A harmonic development of the tide generating potential. Bull. d’Inf. Marées Terr. 99.

Tanaka, Y., Miyajima, R., Asai, H., Horiuchi, Y., Kumada, K., Asai, Y., & Ishii, H. (2011). Hydrological gravity response detection using a gPhone below- And aboveground. Earth, Planets and Space, 65(2011), 59–66. https://doi.org/10.5047/eps.2012.06.012

Turc, L., 1961. Evaluation des besoins en eau d'irrigation, évapotranspiration potentielle. Annales Agronomiques 12(1): 13-49.

Valois, R., 2011. Caractérisation structurale de morphologies karstiques superficielles et suivi temporel de l'infiltration à l'aide des méthodes électriques et sismiques. Sisyphe. Paris, Université Pierre et Marie Curie: 244.

van Beynen, P. E., M. A. Niedzielski, E. Bialkowska-Jelinska, K. Alsharif & J. Matusick, 2012. Comparative study of specific groundwater vulnerability of a karst aquifer in central Florida. Applied Geography 32(2): 868-877.

Van Camp, M., P. Meus, Y. Quinif, O. Kaufman, M. Van Ruymbeke, M. Vandiepenbeeck & T. Camelbeek, 2006a. Karst aquifer investigation using absolute gravity. Eos Transactions 87(30): pp. 298.

Van Camp, M., M. Vanclooster, O. Crommen, T. Petermans, K. Verbeeck, B. Meurers, T. van Dam & A. Dassargues, 2006b. Hydrogeological investigations at the Membach station, Belgium, and application to correct long periodic gravity variations. Journal of Geophysical Research 111: B10403.

Van Camp, M., Viron, O., Watlet, A., Meurers, B., Francis, O., & Caudron, C., 2017. Geophysics From Terrestrial Time-Variable Gravity Measurements. Reviews of Geophysics.

Wenzel, H.-G., 1996. The Nanogal software: earth tide data processing package ETERNA 3.30. Bulletin d'Informations des Marees Terrestres 124: 9425–9439.

Williams, P. W., 2008. The role of the epikarst in karst and cave hydrogeology: a review. International Journal of Speleology 37(1): 1-10.

Vouillamoz, J. M., Legchenko, A., Albouy, Y., Bakalowicz, M., Baltassat, J. M., & Al-Fares, W. (2003). Localization of saturated karst aquifer with magnetic resonance sounding and resistivity imagery. Groundwater, 41(5), 578-586.

Wu, J., A. G. Journel & T. Mukerji, 2006. Establishing spatial pattern correlations between water saturation time-lapse and seismic amplitude time-lapse. Journal of Canadian Petroleum Technology 45(11): 15-20.

Zhang, Z., X. Chen, A. Ghadouani & S. Peng, 2011. Modelling hydrological processes influenced by soil, rock and vegetation is a small karst basin of southwest China. Hydrological Processes 25: 2456-2470.

Appendix 1 : *Results of the least square inversion for each site and each time periods. Results at BESS site is represented for each thickness. Strategy stands for the number of gravity measurements at the reference gravity points depending on the strategy (long or short). Recharge periods are indicated by the gray color.*

Site	***Date***	***Strategy.***	***Calibration correction factor***	***ΔgS2D (mGal)***	***σ STD (mGal)***
SEOU	t_1 : 24/02/2010	short	0.999377	-3.897	0.0014
	t_2 : 26/08/2010	short	0.999337	-3.914	0.0036
	t_3 : 07/10/2010	long	0.999337	-3.910	0.0014
	t_4 : 03/05/2011	long	0.999569	-3.906	0.0014
	t_5 : 13/09/2011	long	0.999569	-3.909	0.0014
BESS (0,12m)	t_1 : 01/03/2010	short	0.999377	-1.523	0.0014
	t_2 : 24/08/2010	short	0.999337	-1.537	0.0028
	t_3 : 01/10/2010	long	0.999337	-1.531	0.0014
	t_4 : 05/05/2011	long	0.999569	-1.528	0.0022
	t_5 : 06/09/2011	long	0.999569	-1.537	0.0014
BESS 12, 23m)	t_1 : 01/03/2010	short	0.999377	-1.320	0.0014
	t_2 : 24/08/2010	short	0.999337	-1.320	0.0022
	t_3 : 01/10/2010	long	0.999337	-1.322	0.0014
	t_4 : 05/05/2011	long	0.999569	-1.317	0.0020
	t_5 : 06/09/2011	long	0.999569	-1.320	0.0014
BESS (23, 41m)	t_1 : 01/03/2010	short	0.999377	-1.724	0.0022
	t_2 : 24/08/2010	short	0.999337	-1.724	0.0022
	t_3 : 01/10/2010	long	0.999337	-1.728	0.0014
	t_4 : 05/05/2011	long	0.999569	-1.726	0.0010
	t_5 : 06/09/2011	long	0.999569	-1.727	0.0014
BESS (41, 58m)	t_1 : 01/03/2010	short	0.999377	-1.277	0.0028
	t_2 : 24/08/2010	short	0.999337	-1.275	0.0028
	t_3 : 01/10/2010	long	0.999337	-1.272	0.0014
	t_4 : 05/05/2011	long	0.999569	-1.275	0.0014
	t_5 : 06/09/2011	long	0.999569	-1.273	0.0014